Biochemical and Biophysical Research Communications 452 (2014) 629–635

Contents lists available at ScienceDirect

Biochemical and Biophysical Research Communications

journal homepage: www.elsevier.com/locate/ybbrc

Naringin prevents ovariectomy-induced osteoporosis and promotes osteoclasts apoptosis through the mitochondria-mediated apoptosis pathway

Fengbo Li [a,b,1], Xiaolei Sun [a,1], Jianxiong Ma [a], Xinlong Ma [a,*], Bin Zhao [a], Yang Zhang [a], Peng Tian [a], Yanjun Li [b], Zhe Han [a]

[a] Tianjin Institute of Orthopedics in Traditional Chinese and Western Medicine, No. 155, Munan Road, Tianjin TJ 300050, China
[b] Graduate School of Tianjin Medical University, No. 22, Qixiangtai Street, Heping District, Tianjin 300070, China

ARTICLE INFO

Article history:
Received 18 August 2014
Available online 30 August 2014

Keywords:
Naringin
Osteoporosis
Apoptosis
Osteoclast

ABSTRACT

Naringin, the primary active compound of the traditional Chinese medicine *Rhizoma drynariae*, possesses many pharmacological activities. The present study is an effort to explore the anti-osteoporosis potential of naringin *in vivo* and *in vitro*. *In vivo*, we used ovariectomized rats to clarify the mechanisms by which naringin anti-osteoporosis. *In vitro*, we used osteoclasts to investigate naringin promotes osteoclasts apoptosis. Naringin was effective at enhancing BMD, trabecular thickness, bone mineralization, and mechanical strength in a dose-dependent manner. The result of RT-PCR analysis revealed that naringin down-regulated the mRNA expression levels of BCL-2 and up-regulated BAX, caspase-3 and cytochrome C. In addition, naringin significantly reduced the bone resorption area *in vitro*. These findings suggest that naringin promotes the apoptosis of osteoclasts by regulating the activity of the mitochondrial apoptosis pathway and prevents OVX-induced osteoporosis in rats.

1. Introduction

Osteoporosis is a common disease worldwide and is characterized by decreased bone mineral density (BMD) and progressive destruction of bone microstructure, resulting in increased bone fragility and risk of fracture [1]. Many factors can lead to osteoporosis, such as estrogen deficiency, hereditary, nutritional deficiencies, chronic diseases, and aging. Estrogen deficiency is the primary cause of osteoporosis in postmenopausal women. Postmenopausal osteoporosis osteoclast activity exceeds osteoblast activity [2]. Osteoporosis increases porosity and decreases bone strength and bone structural integrity [3,4]. These changes can be observed on micro-CT, histologically and in the serum. The serum concentration of CTX-1 and the OC are markers of osteoclast bone-resorbing and osteoblast bone-forming activities, respectively [5,6].

Osteoclasts are multinucleated cells that branch from the monocyte or macrophage lineage. The receptor activator of the nuclear factor-κB ligand (RANKL) and macrophage-colony stimulating factor (M-CSF) are key factors for osteoclast differentiation [7,8]. The major role of M-CSF is the induction of the pre-osteoclast expression of RANK, which is a receptor of RANKL. In this study, the RAW264.7 cells were able to differentiate into osteoclasts upon induction by RANKL in the absence of M-CSF. The cell apoptosis pathway is activated by a variety of factors, including physical, chemical and biological factors, which can activate either the death receptor pathway (Fas, TNF) or mitochondrial apoptosis pathway [9,10]. Many drugs, such as bisphosphonate, promote the apoptosis of osteoclasts to act as anti-osteoporosis agents [11].

Currently, bisphosphonates are the most commonly used drugs for osteoporosis. Bisphosphonates are inhibitors of bone resorption that can reduce bone resorption and decrease bone turnover [12]. However, studies have reported that bisphosphonates can cause many side effects, including osteonecrosis, atypical femoral fractures, esophageal cancer, and renal dysfunction [13,14]. Therefore, many scientists have begun to study natural medicine, which is believed to be healthier and safer for the treatment.

Naringin is a polymethoxylated flavonoid that exhibits a variety of biological and pharmacological effects. Studies have reported that naringin promotes the proliferation of rat osteoblast-like cells (UMR-106), mouse osteoblastic cells and human mesenchymal stem cell differentiation [15,16]. Although some studies have con-

* Corresponding author. Address: Tianjin Institute of Orthopedics in Traditional Chinese and Western Medicine, Tianjin Hospital, No. 155, Munan Road, Tianjin TJ 300050, China. Fax: +86 13752063935.
E-mail address: gengxiao502@163.com (X. Ma).
[1] These authors contributed equally to this work.

http://dx.doi.org/10.1016/j.bbrc.2014.08.117
0006-291X/

firmed that naringin can improve bone mass in osteoporosis rats [17], the mechanism by which naringin exhibits anti-osteoporosis activity, especially the effect of naringin on osteoclasts apoptosis, remains unclear. Therefore, the purpose of this study was to evaluate the effect of naringin anti-osteoporosis activity induced by ovariectomy and to test this hypothesis on the influence of naringin on osteoclasts apoptosis.

2. Materials and methods

2.1. Animals

Healthy 6-month-old female Sprague–Dawley rats (Body weight, 230 ± 10 g) were provided by the Experimental Animal Center of Tianjin Hospital. The experimental animals received humane care, and the study protocols conformed to the guidelines of Tianjin Hospital Ethics Committee. The animals were housed in an air-conditioned environment (22 ± 2 °C) with a 12-h light/dark cycle (7:00–19:00) and were allowed free access to food pellets and water throughout the experiment. Sixty rats were randomly divided into six groups (10/group), and five groups were subjected to bilateral removal of the ovaries (OVX). The rats in the sham group were subjected to incision and sutured without removal of the ovaries. After 60 days of surgery, the five OVX group were treated orally with vehicle (H_2O), naringin (40, 100, 200 mg/kg/day), or 17-β estradiol (22.5 μg/kg/day) for 60 days. The sham group was treated orally with H_2O only. To obtain dynamic parameters of callus formation and remodeling, tetracycline (25 mg/kg) was injected intramuscularly at 10 and 3 days before sacrifice. Blood was collected from the heart under ketamine anesthesia. After centrifugation, serum was obtained and kept at −80 °C until further analysis. The femurs were dissected, and 5 right femurs in each group were fixed with 75% ethanol stored at 4 °C for decalcification; the remaining femur was stored in phosphate-buffered saline at −20 °C until the analysis of BMD, micro-CT and femoral mechanical testing.

2.2. BMD analysis

The BMD of three representative right femurs in each group ($n = 5$) were measured by dual-energy X-ray absorptiometry (DEXA) (LUNAR DPXIQ, GE Healthcare, USA).

2.3. Micro-CT analysis

After DEXA measurements, the trabecular bone microarchitecture of the distal right femoral metaphysis was measured using a microtomography scanner (SkyScan 1076, Kontizh, Belgium) with a slice thickness of 21 μm and the voxel resolution of 22 μm^3. The volume of interest (VOI) was selected as a region 25–125 slices away from the distal femur growth plate. The 3D images were obtained for visualization and display. Bone morphometric parameters, including bone volume over total volume (BV/TV), trabecula number (Tb.N), and trabecula thickness (Tb.Th), were obtained by analyzing the VOI.

2.4. Histological and fluorescent analysis

After fixation in 75% alcohol for 7 days, the right femur (5/group) specimens were dehydrated in graded ethanol and embedded in methylmethacrylate. Seven micron-thick sections were obtained along the sagittal plane of the femur using tungsten carbide blades (Leica SP1600, Germany). Finally, the sections were stained in Giemsa and von Kossa for observation. Osteoporosis dynamic parameters, abbreviations, formulas and units were measured with the method described by Stevenson and Parfitt. The parameters were analyzed by Image-Pro Plus 6.0 software.

2.5. Mechanical testing

The mechanical strength of the shaft and neck of left femur (10/group) was measured with the method described by Ma and Fu [18]. Five left femurs were used to analyze the mechanical strength of the femur midshaft, and another was used to analyze the femoral neck. A vertical load was applied to the left midshaft of the femur and the top of the left femoral head using the Endura TELELF 3200 mechanical testing instrument (Bose Corporation, USA). Mechanical loading speed was maintained at a constant displacement speed of 5 mm/min until the midshaft of the femur and femoral neck fractured. The fracture load was recorded.

2.6. Serum analysis

Serum OC and CTX-1 were measured using an ELISA assay kit (blue gene, China) to study the levels of osteoblastic and osteoclastic markers (8/group).

2.6. Osteoclast differentiation of RAW 264.7 cells

RAW 264.7 cells were purchased from Institute of Basic Medicine of Peking Union Medical College (Beijing, China). RAW264.7 cells were grown in high glucose Dulbecco minimum essential medium supplemented with 10% heat-inactivated fetal bovine serum (FBS) and 1% penicillin–streptomycin at 37 °C in a humidified atmosphere of 95% air and 5% CO_2. RAW 264.7 cells (1×10^4, in a 24-well plate) were induced by RANKL (100 ng/ml) for 5 days. The culture medium was replaced every 48 h. A 20 ng/ml concentration of naringin was added to these cultures for 7 days. The number of osteoclasts was measured using a TRAP staining kit (sigma, USA) under a light microscope.

2.7. Resorption pit assay

RAW 264.7 cells were seeded on bovine cortical bone slices at a density of 20,000 cells/cm^2. The cells were cultured with media containing 100 ng/mL RANKL over the course of 5 days. The culture medium was replaced every 48 h. The cells were removed from the bovine cortical bone slices by sonication in 0.1 N NaOH for 5 min, fixed with 2.5% glutaraldehyde for 30 min, subjected to ethanol gradient dehydration, drying and spraying, and observed with SEM.

2.8. Analysis of osteoclast apoptosis

The effects of naringin on osteoclasts apoptosis was quantified using the Annexin V-FITC apoptosis detection kit (BD Biosciences, Franklin Lakes, NJ, USA). Osteoclasts were treated with naringin (20 ng/ml) for 7 days and then washed twice with PBS and gently re-suspended in Annexin V binding buffer at a concentration of 1×10^6 cells/ml. The osteoclasts (1×10^5 cells, 100 μl) were added to a 5-ml flow tube, and 5 μl Annexin V-FITC and 5 μl propidium iodide (PI) were transferred. The cells were incubated for 15 min at room temperature (25 °C) in the dark and analyzed by flow cytometry (BD FACSCalibur, US) within 1 h. The early apoptotic cells were record.

2.9. Quantitative real-time PCR

After treatment with naringin for 3 days, the cells were washed twice with PBS and collected. Total RNA was extracted using TRIzol

(Invitrogen, USA), following the instructions of the manufacturer. cDNA was synthesized from total-RNA using All-in-One™ First-Strand cDNA Synthesis Kit (GeneCopoeia., USA) and oligo (dT) primers for the analysis of osteoclast apoptosis-related genes, including the following: BCL-2, Forward 5′-ACGGGGTGAACTG GGGGAGG-3′ and Reverse 5′-GCATGCTGGGGCCGTACAGT-3′; BAX, Forward 5′-GATGGACGGGTCCGGAGA-3′ and Reverse 5′-CTCAGCCC ATCTTCTTCCAG-3′; Caspase-3, Forward 5′-TTCAGAGGGGATCGTT GTAGAAGTC-3′ and Reverse 5′-CAAGCTTGTCGGCATACTGTTTCA G-3′; Cytc, Forward 5′-TGGGCGGAAGACAGGTCA-3′ and Reverse 5′-TCCAGGGATGTACTTCTTGGGAT-3′; and β-actin, Forward 5′-GG GAAATCGTGCGTGACATT-3′ and Reverse 5′-GGAACCGCTCATTGCC AAT-3′. The reaction conditions were set according to the kit instructions. After completion of the reaction, the amplification curve and melting curve were analyzed. Gene expression values are represented using the $2^{-\Delta\Delta Ct}$ method.

2.10. Statistical analysis

Data are presented as the mean value ± SD. Statistical analysis was performed with ANOVA using SPSS16.0 software. *P*-values < 0.05 were considered statistically significant.

3. Results

3.1. BMD

The right femoral BMD values in OVX rats treated with naringin and estrogen orally increased significantly (Fig. 1E). Among the treatment concentrations of naringin, 200 mg/kg appeared to be the optimal dosage for preserving BMD ($P < 0.01$, Fig. 1E).

3.2. Micro-CT

Three-dimensional images of the right distal femur with differences in the trabecular microarchitecture among the six groups are presented in Fig. 1A. Analyses of the data from the right distal femur revealed that OVX rats exhibited significantly ($P < 0.01$) lower trabecular BV/TV, Tb.N and Tb.Th, compared with the sham rats. There were significant increases in the BV/TV ratio (Fig. 1B), Tb.N (Fig. 1C) and Tb.Th (Fig. 1D) in the 100 and 200 mg/kg naringin treatment groups after 60 days of naringin gavages, and the 200 mg/kg dose again produced the optimal therapeutic effect.

3.3. Histological and fluorescent analysis

Undecalcified histological images are presented in Fig. 2. After treatment with naringin for 60 days, more calluses were observed in the naringin group compared with the OVX group. Compared with the OVX group, the study revealed that 100 and 200 mg/kg naringin increased osteoblast perimeter (Ob.Pm) and decreased osteoclast perimeter (Oc.Pm). It showed that decreased Ob.Pm and Oc.Pm in E_2 group. Naringin increase Osteoid perimeter (O.Pm). The naringin treatment increased the mineral apposition rate (MAR) compared with the control. However, E_2 treated resulted in the lowest MAR.

3.4. Mechanical testing

The average maximum fracture loading to the femoral midshaft (Fig. 3A) and left femoral neck (Fig. 3B) was lower in the OVX control group compared with the naringin and 17-β estradiol groups. Naringin (200 and 100 mg/kg) and 17-β estradiol significantly increased the average maximum fracture loading of the left femoral neck and femoral midshaft. There was no significant difference between the 40 mg/kg naringin group and the OVX groups.

3.5. Serum analysis

Four months after the operation, the OVX group exhibited significant increases in serum CTX-1 and OC activities compared with the sham-treated rats. The results demonstrated that 100 and 200 mg/kg naringin significantly enhanced the serum OC (Fig. 3C) and decreased the serum CTX-1 (Fig. 3D) compared with the OVX group rats, whereas serum OC and CTX-1 were reduced in the estrogen group.

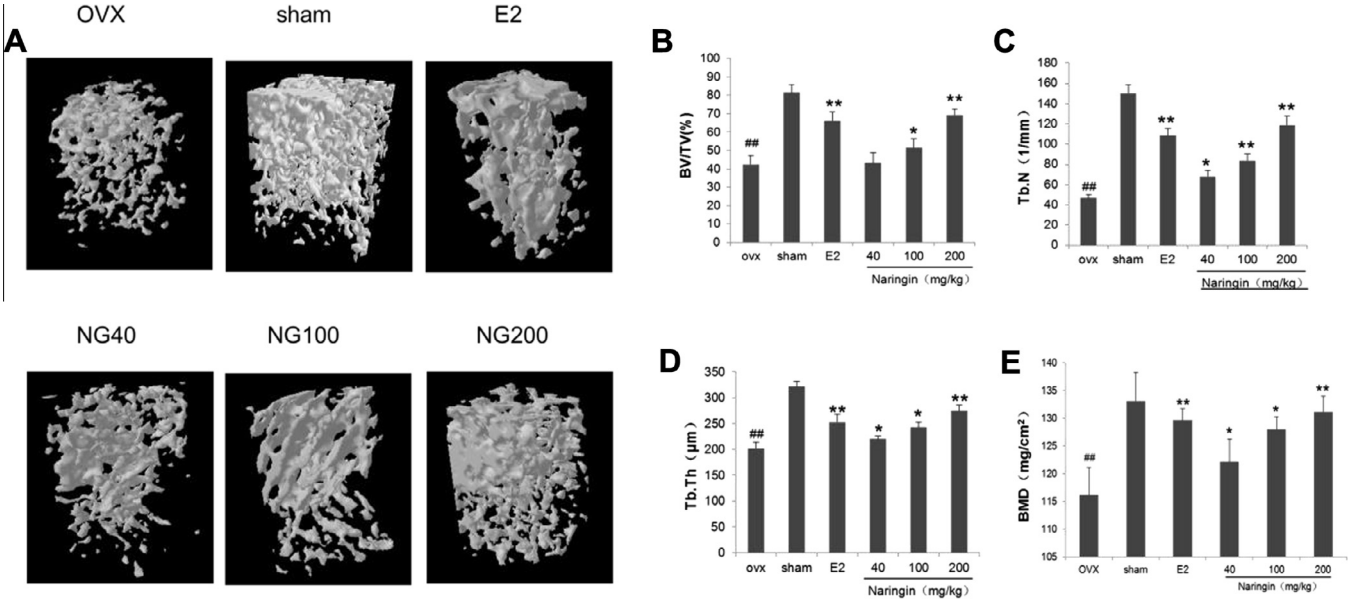

Fig. 1. (A) Representative sample from each group: 3D architecture of trabecular bone within the distal femoral metaphyseal region. Effects of naringin or 17-β estradiol on the trabecular bone volume (B), number of trabeculae (C), and thickness of the trabeculae (D) of the distal femoral metaphysic in OVX rats by microtomography analysis. (E) BMD by DEXA examination. Values are means ± standard deviation, $n = 5$. $^{*}P < 0.05$, $^{**}P < 0.01$ vs. OVX group; $^{\#}P < 0.01$, $^{\#\#}P < 0.01$ vs. SHAM group as evaluated by ANOVA.

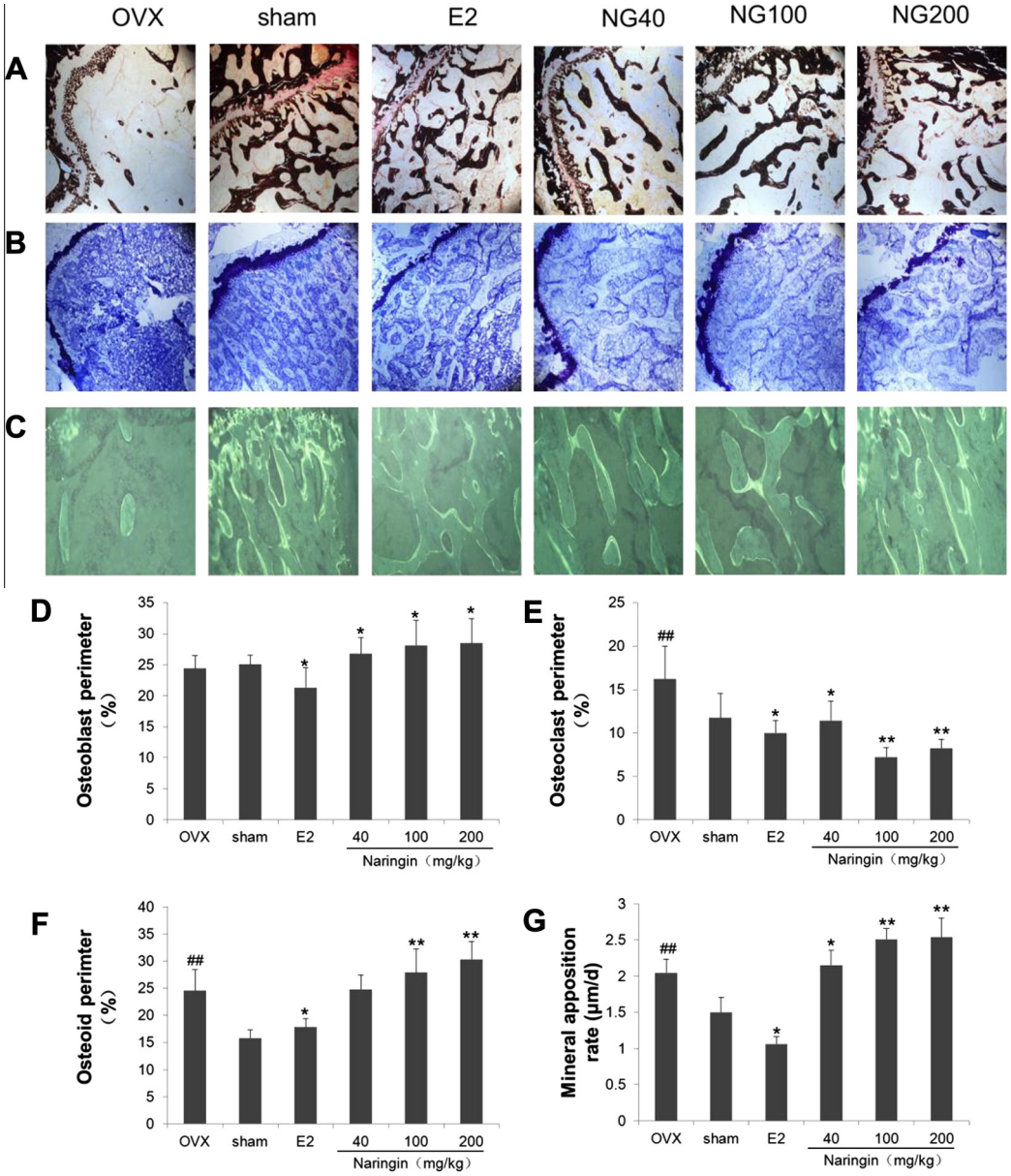

Fig. 2. Undecalcified histological sections, stained with von Kossa (A) and Giemsa (B), of the sagittal plane through the distal of femur (magnification, ×100). (C) Undecalcified sections observed under a fluorescence microscopy demonstrating the tetracycline fluorescence (magnification, ×200). (D) Statistical analysis of the osteoblast perimeter. (E) Statistical analysis of the osteoclast perimeter. (F) Statistical analysis of the osteoid perimeter. (G) Statistical analysis of the mineral apposition rate. Values are means ± standard deviation, $n = 5$. $^{*}P < 0.05$, $^{**}P < 0.01$ vs. OVX group; $^{\#}P < 0.01$, $^{\#\#}P < 0.01$ vs. SHAM group as evaluated by ANOVA.

3.6. Naringin inhibits the number of TRAP-positive osteoclasts and their resorption activity

Compared with the control group, the number of mature osteoclasts was decreased in the naringin group (Fig. 4A). We next evaluated the effect of naringin on osteoclast resorption. RAW 264.7 cells were plated on bovine cortical bone slices and induced with RANKL (100 ng/ml) for 5 days. The results demonstrated that treatment with naringin (20 ng/ml) significantly decreased the resorbed area compared with treatment with RANKL alone (Fig. 4B).

3.7. Naringin promotes osteoclast apoptosis

The activity of early apoptotic cells was enhanced in the naringin group (24.18 ± 6.68%) compared with the control group (14.32 ± 4.00%). These results indicate that naringin increased osteoclast apoptosis (Fig. 4C).

3.8. The effect of naringin on the expression of osteoclast apoptosis-related genes

Compared with the control group, the expression of caspase-3 and cytochrome C was increased in the naringin group. BCL-2 mRNA expression was down-regulated, and BAX mRNA expression was up-regulated. The BCL-2/BAX ratio in the naringin group decreased compared with the control group. These results suggest that naringin plays an important role in osteoclast apoptosis (Fig. 4D–F).

4. Discussion

In the present study, we have demonstrated that naringin enhances bone mass and bone strength in a rat model of osteoporosis by altering bone metabolism. This study also indicates that naringin promotes the apoptosis of osteoclasts by mitochondrial

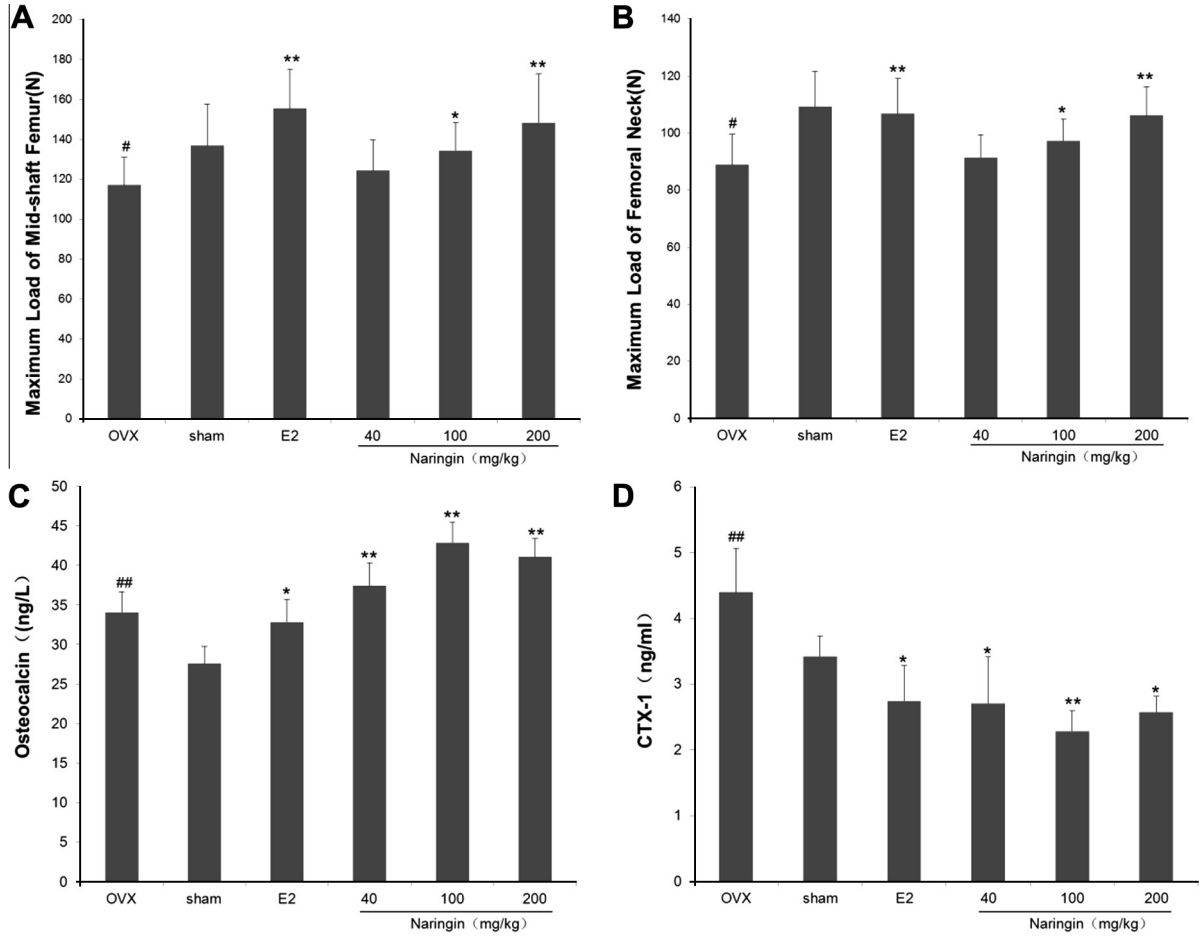

Fig. 3. Effects of 60-day treatment with naringin or 17-β estradiol on the mechanical strength of midshaft femur (A) and femoral neck (B) of OVX rats. (C) Statistical analysis of the osteocalcin. (D) Statistical analysis of the CTX-1. Values are presented as the mean ± standard deviation, $n = 10$. $^{*}P < 0.05$, $^{**}P < 0.01$ vs. OVX group; $^{\#}P < 0.01$, $^{\#\#}P < 0.01$ vs. SHAM group as evaluated by ANOVA.

apoptosis pathway *in vitro*. This study used ovariectomized rats as a model to analyze the efficacy of naringin in the treatment of postmenopausal osteoporosis. The analysis of BMD and micro-CT demonstrated that BMD, BV/TV, Tb.N, and Tb.Th were significantly decreased in the OVX rats 60 days after surgery. Although BMD was recognized as an important predictor of osteoporosis fractures, studies have reported only 10–53% compliance with BMD criteria to diagnose osteoporosis in the presence of osteoporotic fractures [19]. However, micro-CT voxel-based test unit is able to detect lesions and structures in bone early [20]. Our results demonstrated that sixty days after treatment with naringin and estrogen, the BMD, BV/TV, Tb.N, and Tb.Th were significantly increased compared with the OVX rats. In contrast, Tb.Sp in the femurs of rats in the naringin and estrogen group was significantly decreased compared with the OVX group. The preservation of trabecular microarchitecture significantly contributes to bone strength and may reduce fracture risk irrespective of BMD [21]. In the present study, we observed that naringin significantly improved the average maximum fracture loading to the midshaft of the femora and the femoral necks in OVX rats. It is worth noting that the 200 mg/kg naringin group exhibited a femoral neck and midshaft strength similar to the estrogen group.

Tetracycline is able to specifically bind calcium used in decalcification and can thus be used to measure multiple parameters of bone tissue dynamics [22]. To counter the impact of estrogen on bone, negative feedback increased the number and function of osteoblasts in OVX rats. The results indicate that fluorescently labeled, osteoid width and resorption surfaces were increased in the OVX group compared with the sham group. This study demonstrates that treatment with naringin significantly increased the ratio of fluorescence marker, the osteoid width, the osteoclast surface area, the mineral apposition rate and the mineralization lag time. Additionally, the osteoblast surface was decreased. The results suggested that naringin both promotes bone formation and inhibits bone resorption.

The CTX-1 plasma activity and the OC are markers of osteoclast bone resorption and bone formation, respectively, and are reportedly increased in OVX animals relative to sham-operated animals [5,6].Treatment with naringin dose-dependently decreases CTX-1 and serum Ca/P levels and increases plasma OC. These results suggest that naringin ameliorated bone loss induced by OVX by inhibiting bone resorption and enhancing bone formation. Studies have reported that naringin promotes the differentiation and proliferation of osteoblasts [23,24]. Our previous experiments also confirmed that naringin (20 ng/ml) could promote the expression of OCN, Runx 2 and Col I *in vitro*. This study demonstrates that naringin promotes osteoclast apoptosis in RAW264.7 cells induced by RANKL *in vitro*.

Mature osteoclasts are terminally differentiated cells. The life span of osteoclasts is short, and the cells undergo spontaneous apoptosis [25], through the activation of the death receptor pathway (Fas, TNF) or mitochondrial apoptosis pathway [26,10]. The latter is achieved by regulating the expression of the anti-apoptotic protein BCL-2 and the pro-apoptotic protein BAX. Cytochrome C

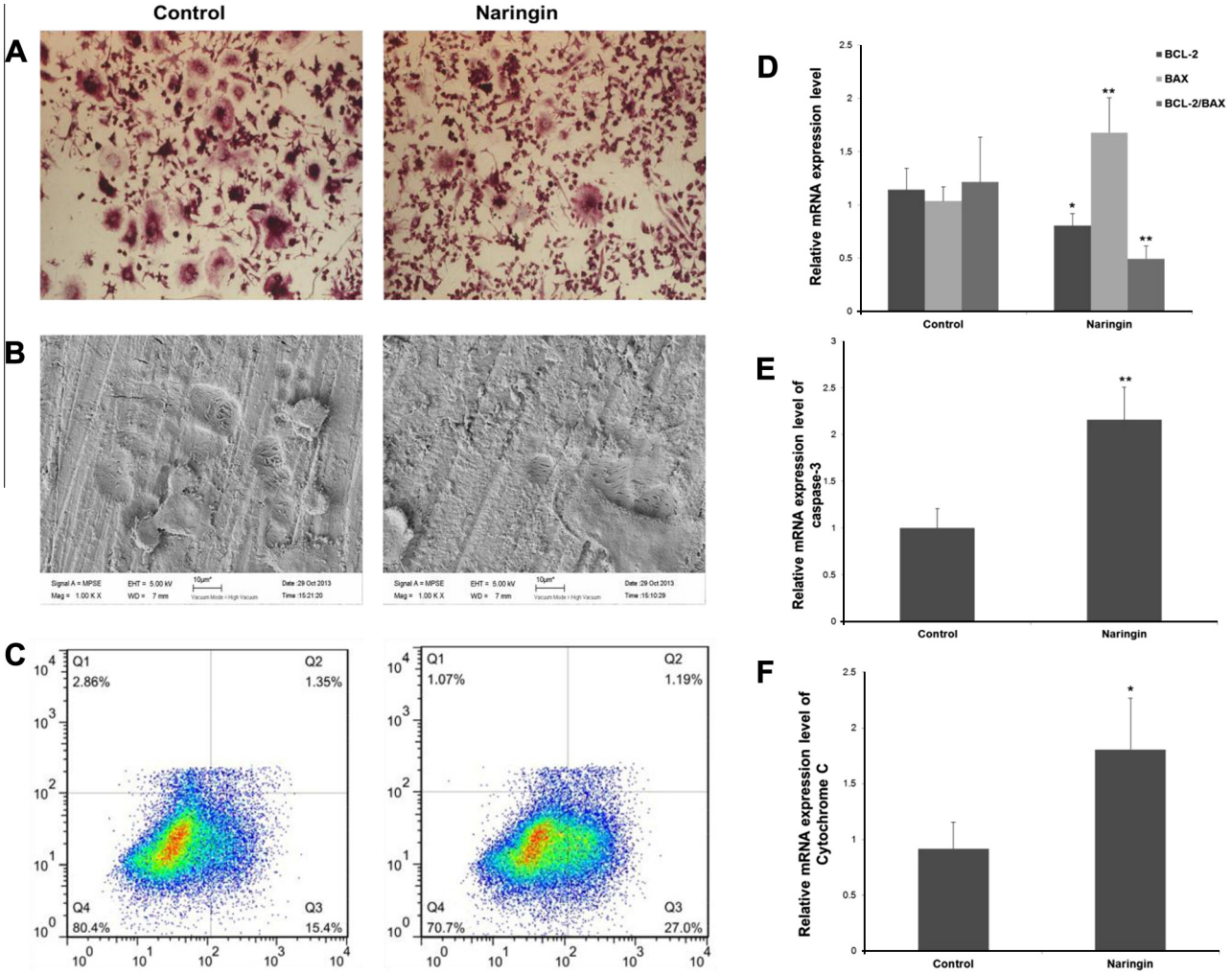

Fig. 4. Effect of naringin (20 ng/ml) treatment on the number of multinucleated TRAP-positive cells (A) and on the resorbed area (B). C Osteoclasts were treated with naringin (20 ng/ml) to measure the activity of early apoptotic cells (C). Representative images are presented. The expression levels of BCL-2/BAX (D), caspase-3 (E), and cytochrome C (F) were measured by RT-PCR. All values are presented as the mean ± standard deviation, $n = 6$. $^{*}P < 0.05$, $^{**}P < 0.01$ vs. OVX group as evaluated by ANOVA.

and other pro-apoptotic factors are released into the cytoplasm downstream of mitochondrial membrane permeability, which is regulated by the ratio between anti-apoptotic factors (BCL-2) and pro-apoptotic factors (BAX).

Apoptosis-related Bcl-2 family member genes are key regulators of apoptosis through the following mechanisms: inhibition of oxygen free radicals, control of intracellular Ca^{2+} influx, inhibition of the release of cytochrome C, and inhibition of p53 and c-myc induced apoptosis. The Bcl-2-associated X protein, Bax [27], and BCL-2 are embedded in the mitochondrial membrane, and Bax dimers can enhance mitochondrial membrane permeability. Bcl-2 and Bax can be combined to form a heterodimeric body to prevent the formation of pro-apoptotic Bax dimers. Furthermore, Bcl-2 dimers can inhibit mitochondrial depolarization [28,29]. The release of cytochrome C into the cytoplasm can enhance the combined activity of the apoptosis protease activating factor-1 (APAF-1) and ATP. The activation of the APAF-1 recruitment precursor caspase-9 catalyzes the auto cleavage of pro-caspase-9, which in turn activates the effectors caspase-3, caspase-6 and caspase-7, promoting apoptosis [30,31]. The caspase family of cysteine aspartic proteases plays an important role at the start and finish of cell apoptosis and represents the executors of cellular apoptosis. There are two pathways upstream of caspase activation. The first is mediated by death receptors like Fas or TNFR. The binding of the Fas ligand and Fas receptor promotes the binding of FADD/MORT-1 with the receptors and the subsequent activation of caspase-8, caspase-3 and other downstream caspases. This caspase cascade amplification reaction cleaves protein substrates in the cell. The second apoptotic pathway occurs downstream of pro-apoptotic signals that promote cytochrome C release from the mitochondria into the cytosol, where it combines with APAF-1 and then binds to and activates pro-caspase-9. The downstream activation of caspase-3 initiates the caspase cascade. Caspase-3 responds to a variety of apoptosis-stimulating signals and acts as the ultimate enforcer of cellular apoptotic death, and the activation of caspase-3 represents the irreversible phase of apoptosis [32]. In this study, we confirmed that naringin can down-regulate the mRNA expression of BCL-2 and up-regulate the expression of BAX, thereby decreasing the ratio of BCL-2/BAX. Naringin increased the permeability of the mitochondrial membrane and promoted the release of cytochrome C and other pro-apoptotic factors into the cytoplasm, thereby initiating the caspase-dependent apoptosis of osteoclasts.

In summary, this study suggests that naringin promotes osteoclast apoptosis and inhibits osteoclast resorption *in vitro*. We also observed that 200 mg/kg of naringin exhibited the best therapeutic effects *in vivo*. The results demonstrated that the oral administration of naringin effectively increased BMD, bone volume, and the

trabecular thickness maximum load. Therefore, naringin might serve as a potential alternative medicine in the treatment of osteoporosis.

Acknowledgments

This study was funded by the Public Health Bureau of Science and Technology of Tianjin, China (No. 2011KZ57) and the Traditional Chinese Medicine Administration of Tianjin, China (No. 13123).

References

[1] J. Berecki-Gisolf, M. Spallek, R. Hockey, A. Dobson, Height loss in elderly women is preceded by osteoporosis and is associated with digestive problems and urinary incontinence, Osteoporosis Int. 21 (2010) 479–485.
[2] S.D. Brincat, M. Borg, G. Camilleri, J. Calleja-Agius, The role of cytokines in postmenopausal osteoporosis, Minerva Ginecol. 66 (2014) 391–407.
[3] C.Y. Li, C. Price, K. Delisser, P. Nasser, D. Laudier, M. Clement, K.J. Jepsen, M.B. Schaffler, Long-term disuse osteoporosis seems less sensitive to bisphosphonate treatment than other osteoporosis, J. Bone Miner. Res. 20 (2005) 117–124.
[4] E.A. Zimmermann, E. Schaible, H. Bale, H.D. Barth, S.Y. Tang, P. Reichert, B. Busse, T. Alliston, J.W. Ager, R.Q.O. Ritchie 3rd, Age-related changes in the plasticity and toughness of human cortical bone at multiple length scales, Proc. Natl. Acad. Sci. USA 108 (2011) 14416–14421.
[5] K.H. Yoon, D.C. Cho, S.H. Yu, K.T. Kim, Y. Jeon, J.K. Sung, The change of bone metabolism in ovariectomized rats: analyses of microCT scan and biochemical markers of bone turnover, J. Korean Neurosurg. Soc. 51 (2012) 323–327.
[6] W. Qi, Y.B. Yan, W. Lei, et al., Prevention of disuse osteoporosis in rats by *Cordyceps sinensis* extract, Osteoporosis Int. 23 (2012) 2347–2357.
[7] W.J. Boyle, W.S. Simonet, D.L. Lacey, Osteoclast differentiation and activation, Nature 423 (2003) 337–342.
[8] J.W. Quinn, M.T. Gillespie, Modulation of osteoclast formation, Biochem. Biophys. Res. Commun. 328 (2005) 739–745.
[9] T. Miyazaki, Role of mitochondria in osteoclast function, Clin. Calcium 23 (2013) 1577–1583.
[10] G. Kroemer, L. Galluzzi, C. Brenner, Mitochondrial membrane permeabilization in cell death, Physiol. Rev. 87 (2007) 99–163.
[11] K. Abe, Y. Yoshimura, Y. Deyama, T. Kikuiri, T. Hasegawa, K. Tei, H. Shinoda, K. Suzuki, Y. Kitagawa, Effects of bisphosphonates on osteoclastogenesis in RAW264. 7 cells, Int. J. Mol. Med. 29 (2012) 1007–1015.
[12] B. Eslami, S. Zhou, I. Van Eekeren, M.S. LeBoff, J. Glowacki, Reduced osteoclastogenesis and RANKL expression in marrow from women taking alendronate, Calcif. Tissue Int. 88 (2011) 272–280.
[13] R.D. Turgeon, S.S. Yeung, Fracture risk and zoledronic acid in men with osteoporosis, N. Engl. J. Med. 367 (2012) 1714–1723.
[14] T. Soda, R. Fukumoto, T. Hayashi, D. Oka, N. Fujimoto, T. Koide, A case of prostate cancer associated with bisphosphonate-related osteonecrosis of the jaw followed by retropharyngeal abscess, Hinyokika Kiyo 59 (2013) 587–591.
[15] W.Y. Pang, X.L. Wang, S.K. Mok, W.P. Lai, H.K. Chow, P.C. Leung, X.S. Yao, M.S. Wong, Naringin improves bone properties in ovariectomized mice and exerts oestrogen-like activities in rat osteoblast-like (UMR-106) cells, Br. J. Pharmacol. 159 (2010) 1693–1703.
[16] P. Zhang, K.R. Dai, S.G. Yan, W.Q. Yan, C. Zhang, D.Q. Chen, B. Xu, Z.W. Xu, Effects of naringin on the proliferation and osteogenic differentiation of human bone mesenchymal stem cell, Eur. J. Pharmacol. 607 (2009) 1–5.
[17] M. Wei, Z. Yang, P. Li, Y. Zhang, W.C. Sse, Anti-osteoporosis activity of naringin in the retinoic acid-induced osteoporosis model, Am. J. Chin. Med. 35 (2007) 663–667.
[18] Z. Ma, Q. Fu, Comparison of the therapeutic effects of yeast-incorporated gallium with those of inorganic gallium on ovariectomized osteopenic rats, Biol. Trace Elem. Res. 134 (2010) 280–287.
[19] L.M. McNamara, Perspective on post-menopausal osteoporosis: establishing an interdisciplinary understanding of the sequence of events from the molecular level to whole bone fractures, J. R. Soc. Interface 7 (2010) 353–372.
[20] S.K. Boyd, P. Davison, R. Müller, J.A. Gasser, Monitoring individual morphological changes over time in ovariectomized rats by in vivo micro-computed tomography, Bone 39 (2006) 854–862.
[21] M.P. Akhter, G.K. Alvarez, D.M. Cullen, R.R. Recker, Recker Disuse-related decline in trabecular bone structure, Biomech. Model. Mechanobiol. 10 (2011) 423–429.
[22] P.A. Revell, Histomorphometry of bone, J. Clin. Pathol. 36 (1983) 1323–1331.
[23] N. Li, Y. Jiang, P.H. Wooley, Z. Xu, S.Y. Yang, Naringin promotes osteoblast differentiation and effectively reverses ovariectomy-associated osteoporosis, J. Orthop. Sci. 18 (2013) 478–485.
[24] L. Li, Z. Zeng, G. Cai, Comparison of neoeriocitrin and naringin on proliferation and osteogenic differentiation in MC3T3-E1, Phytomedicine 18 (2011) 985–989.
[25] S.L. Teitelbaum, Bone resorption by osteoclasts, Science 289 (2000) 1504–1508.
[26] K.M. Debatin, P.H. Krammer, Death receptors in chemotherapy and cancer, Oncogene 23 (2004) 2950–2966.
[27] J.M. Adams, Cory S, Bcl-2-regulated apoptosis: mechanism and therapeutic potential, Curr. Opin. Immunol. 19 (2007) 488–496.
[28] X.M. Yin, Bid, a BH3-only multi-functional molecule, is at the cross road of life and death, Gene 369 (2006) 7–19.
[29] M. Certo, V. Del Gaizo Moore, M. Nishino, G. Wei, S. Korsmeyer, S.A. Armstrong, A. Letai, S. Korsmeyer, S.A. Armstrong, A. Letai, Mitochondria primed by death signals determine cellular addiction to antiapoptotic BCL-2 family members, Cancer, Cell 9 (2006) 351–365.
[30] E.E. Hellebrand, G. Varbiro, Development of mitochondrial permeability transition inhibitory agents: a novel drug target, Drug Discovery Ther. 4 (2010) 54–61.
[31] R.L. Jilka, B. Noble, R.S. Weinstein, Osteocyte apoptosis, Bone 54 (2013) 264–271.
[32] V. Cryns, J. Yuan, Proteases to die for, Genes Dev. 12 (1998) 1551–1570.